Mon. Not. R. Astron. Soc. **000**, 000–000 (2001)

# Predicting the clustering properties of galaxy clusters detectable for the *Planck* satellite

L. Moscardini[1], M. Bartelmann[2], S. Matarrese[3] and P. Andreani[4]
[1] *Dipartimento di Astronomia, Università di Padova, vicolo dell'Osservatorio 2, I–35122 Padova, Italy*
[2] *Max-Planck-Institut für Astrophysik, Karl-Schwarzschild-Strasse 1, D-85748 Garching, Germany*
[3] *Dipartimento di Fisica G. Galilei, Università di Padova, via Marzolo 8, I–35131 Padova, Italy*
[4] *Osservatorio Astronomico di Padova, vicolo dell'Osservatorio 5, I–35122 Padova, Italy*

20 December 2001

**ABSTRACT**
We study the clustering properties of the galaxy clusters detectable for the *Planck* satellite due to their thermal Sunyaev-Zel'dovich effect. We take the past light-cone effect and the redshift evolution of both the underlying dark matter correlation function and the cluster bias factor into account. A theoretical mass-temperature relation allows us to convert the sensitivity limit of a catalogue into a minimum mass for the dark matter haloes hosting the clusters. We confirm that the correlation length is an increasing function of the sensitivity limits defining the survey. Using the expected characteristics of the *Planck* cluster catalogue, which will be a quite large and unbiased sample, we predict the two-point correlation function and power spectrum for different cosmological models. We show that the wide redshift distribution of the *Planck* survey, will allow to constrain the cluster clustering properties up to $z \approx 1$. The dependence of our results on the main cosmological parameters (the matter density parameter, the cosmological constant and the normalisation of the density power-spectrum) is extensively discussed. We find that the future *Planck* clustering data place only mild constraints on the cosmological parameters, because the results depend on the physical characteristics of the intracluster medium, like the baryon fraction and the mass-temperature relation. Once the cosmological model and the Hubble constant are determined, the clustering data will allow a determination of the baryon fraction with an accuracy of few per cent.

**Key words:** galaxies: clusters: general – cosmology: theory – dark matter – large–scale structure of Universe – cosmic microwave background

## 1 INTRODUCTION

In the standard picture of structure formation based on the gravitational instability paradigm, clusters of galaxies represent the largest gravitationally bound systems in the universe. This is the reason for their cosmological importance. In fact, since the expected displacements from their primordial positions are much smaller than their typical separations, clusters retain the imprint of the main cosmological parameters, which can hopefully be constrained studying their properties. In the past this opportunity has been largely exploited using cluster counts and their redshift evolution (e.g. Eke et al. 1998; Sadat, Blanchard & Oubkir 1998; Viana & Liddle 1999; Borgani et al. 2001; Verde, Haiman & Spergel 2001), obtaining tight constraints on the matter density parameter $\Omega_{0\mathrm{m}}$ and power-spectrum normalisation $\sigma_8$.

Galaxy clusters are also good tracers of the large-scale structure of the Universe. Their clustering signal can easily be detected, even with a relatively small number of objects. In fact, they form in overdense regions of the cosmological density field and are strongly biased. A confirmation that the spatial distribution of galaxy clusters is highly correlated came from the statistical analysis of the first extended optical surveys (Nichol et al. 1992; Croft et al. 1997), which however may be affected by the presence of interloper galaxies. A better identification of galaxy clusters is possible in the X-ray band. Here their emission due to thermal bremsstrahlung from the hot intracluster plasma, is more centrally concentrated because it depends on the square of the baryon density. In the past years the completion of extended catalogues covering a large fraction of the sky allowed the computation of the clustering properties of X-ray selected clusters (Abadi, Lambas & Muriel 1998; Borgani,

Plionis & Kolokotronis 1999; Moscardini et al. 2000a; Collins et al. 2001; Schuecker et al. 2001). The results obtained for different surveys are fairly different, reflecting a strong dependence on the cluster selection criteria (limiting flux or luminosity in a given band) adopted.

It is important to notice that the clustering of galaxy clusters represents an important test for models of structure formation. As shown by numerical simulations, cluster evolution can easily be understood and interpreted, once they are identified as the most massive dark haloes produced by gravitational collapse. As a consequence, one can model their clustering properties starting from the dark halo properties, which can be obtained from an extension of the standard Press-Schechter formalism (e.g. Mo & White 1996). The resulting correlation function depends strongly on cosmology and the primordial power spectrum. In this paper we will use an improved theoretical model (Matarrese et al. 1997), paying particular attention to the redshift evolution of object clustering and to light-cone and selection effects. A treatment of the redshift-space distortions is also included. This model has already been applied recently to compare the existing cluster data (both in the optical and in the X-ray bands) with model predictions, finding further evidence in favour of low-density models (Moscardini et al. 2000b; Moscardini, Matarrese & Mo 2001).

In this context, a new window is now opening to extend the study of the cluster distribution in the microwave band, thanks to the thermal Sunyaev-Zel'dovich (SZ) effect, i.e. the change of the blackbody spectrum of the cosmic radiation background produced by Compton scattering off the hot intracluster medium. Observational data of some individual galaxy clusters have already been obtained, allowing a better morphological study of individual objects. However, at present well-defined surveys required for statistical studies are not available yet, even though several ground-based experiments with this objective are being planned for the near future (e.g. BOLOCAM, AMIBA, CBI, etc.).

The goal of a full-sky survey of SZ clusters will be reached only with space missions. In particular, the *Planck* satellite, which is scheduled for launch in 2007, will detect of order $10^4$ clusters thanks to the optimal choice of filter bands around the frequencies relevant for the SZ effect. This large number of clusters, even if obtained with an angular resolution lower than that of the above-mentioned ground-based bolometer arrays and interferometers, will allow an accurate measurement of the cluster correlation function and constraints on its redshift evolution.

This paper reports on an extended study of the clustering properties of galaxy clusters detectable for the *Planck* satellite. It is worth mentioning that an estimate of the contribution from the correlation among clusters to the angular power spectrum of the cosmic microwave background radiation anisotropy due to fluctuations of the SZ effect has been obtained by Komatsu & Kitayama (1999) using an approach similar to the one applied here (see also Refregier et al. 2000).

The plan of the paper is as follows. In Section 2 we discuss the general characteristics of the objects detectable for *Planck*. Section 3 reviews the theoretical model for the correlation function of SZ galaxy clusters in the framework of different cosmological models. In Section 4 we discuss the implications of the previous results and the possibility of constraining the main cosmological parameters using the future *Planck* observations. Section 5 shows the dependence of the clustering predictions on the characteristics of the intracluster medium, like the baryon fraction and the mass-temperature relation. Conclusions are drawn in Section 6.

## 2 GALAXY CLUSTERS DETECTABLE FOR *PLANCK* THROUGH THERMAL SUNYAEV-ZEL'DOVICH EMISSION

Galaxy clusters can be detected in the microwave regime due to their thermal Sunyaev-Zel'dovich effect. Hot electrons in the intracluster medium Compton-scatter the cold photons of the microwave background and redistribute them towards higher frequencies. The result is a temperature decrement below 218 GHz, and an increment above.

The SZ effect in direction $\vec{\theta}$ is quantified by the Compton-$y$ parameter,

$$y(\vec{\theta}) = \frac{k\sigma_{_T}}{m_e c^2} \int dl \; n_e(\vec{\theta}, l) \; T(\vec{\theta}, l) \; , \qquad (1)$$

where $T$ is the electron temperature, $n_e$ the three-dimensional thermal electron density (hereafter assumed to follow a King profile), and $\sigma_{_T}$ is the Thomson scattering cross section.

Assuming an isothermal distribution of gas and neglecting the background noise (see the following discussion), the total SZ signal received from a cluster is simply the integral over the solid angle covered, i.e.

$$Y \equiv \int d^2 \; \vec{\theta} \; y(\vec{\theta}) = \frac{kT}{m_e c^2} \frac{\sigma_{_T}}{D_d^2} N_e \; , \qquad (2)$$

where $D_d$ is the angular-diameter distance to the cluster, which of course depends on cosmology. The total number of electrons in the cluster $N_e$ can be assumed to be proportional to the virial mass $M$,

$$N_e = \frac{1 + f_H}{2} f_b \frac{M}{m_p} \; , \qquad (3)$$

where $m_p$ is the proton mass, $f_b$ is the baryon fraction of the cluster mass and $f_H$ is the hydrogen fraction of the baryonic mass (here assumed as 76 per cent). Assuming an isothermal gas distribution in virial equilibrium and spherical collapse, it is possible to relate the cluster temperature (in keV) to its mass,

$$T = 6.03 \left( \frac{M}{10^{15} h^{-1} M_\odot} \right)^{2/3} E^{2/3}(z) \left[ \frac{\Delta_{\rm vir}(z)}{178} \right]^{1/3} \; . \qquad (4)$$

The quantity $\Delta_{\rm vir}(z)$ is the mean density of the virialised halo in units of the critical density at redshift $z$, while $E(z)$ is the Hubble constant at redshift $z$ in units of its present value, $E(z) \equiv H(z)/H_0$. The normalisation of the mass-temperature relation is taken from the analysis of hydrodynamical simulations by Mathiesen & Evrard (2001). Using this set of relations, the quantity

$Y$ depends on the cosmological model, and on cluster mass and redshift only, i.e. $Y \equiv Y(M,z)$.

For modelling the cluster population detectable for *Planck* we have to take into account the characteristics of the satellite detector (e.g. Haehnelt 1997; Bartlett 2000; Bartelmann 2001). Its relatively poor angular resolution will not allow most of the cluster population to be resolved (e.g. Aghanim et al. 1997; Hobson et al. 1998). Unresolved clusters below the detection limit will produce a Compton-$y$ background $y_{\rm bg}$. Neglecting background correlations, the average background fluctuation level can be estimated as

$$(\Delta y_{\rm bg})^2 = \int dz \left|\frac{dV}{dz}\right| (1+z)^3 \int dM\, \overline{n}(M,z)\, Y^2(M,z) \quad (5)$$

(e.g. Bartelmann 2001). In the previous expression, $dV$ is the cosmic volume per unit redshift and unit solid angle, and $\overline{n}(M,z)$ is the cluster mass function which can be estimated using the Press-Schechter approach or more recent extensions, see below.

Moreover, the original cluster SZ signal will be convolved by the *Planck* beam profile $w(\vec{\theta})$, which depends on the observing frequency. We assume for our purposes that cluster selection will be mainly performed at the highest frequencies and approximate the beam profile with a Gaussian with r.m.s. $\sigma_w = 5$ arcmin.

We assume that a cluster is detectable for *Planck* if its integrated, beam-convolved Compton-$y$ parameter is larger than a given sensitivity limit, i.e. $\overline{Y} \geq \overline{Y}_{\rm min}$, where

$$\overline{Y} \equiv \frac{1}{2\pi\sigma_w^2} \int d^2\theta \int d^2\theta'\; y(\theta')\; \exp\left[-\frac{(\theta-\theta')^2}{2\sigma_w^2}\right] \; . \quad (6)$$

The external integral covers the solid angle where the signal is large enough to be detected. Using its nominal temperature sensitivity and the solid angle of the beam, the sensitivity limit for *Planck* can conservatively be set to $\overline{Y}_{\rm min} = 3 \times 10^{-4}$ arcmin$^2$ (Bartelmann 2001).

## 3 THE CLUSTERING MODEL

Our model for predicting the clustering properties of the SZ galaxy clusters derives from a method already applied to the study of clusters detected in the X-ray and optical bands (Moscardini et al. 2000a,b; Moscardini, Matarrese & Mo 2001). We will give a brief description of the technique only and refer to the original papers for a more detailed discussion.

Matarrese et al. (1997; see also Moscardini et al. 1998; Yamamoto & Suto 1999; Suto et al. 2000; Hamana et al. 2001) developed an algorithm for describing the clustering on our past light-cone taking into account both the non-linear dynamics of the dark matter distribution and the redshift evolution of the bias factor. The final expression for the observed spatial correlation function $\xi_{\rm obs}$ in a given redshift interval $\mathcal{Z}$ is

$$\xi_{\rm obs}(r) = \frac{\int_{\mathcal{Z}} dz_1 dz_2 \overline{\mathcal{N}}(z_1)\overline{\mathcal{N}}(z_2)\; \xi_{\rm obj}(r;z_1,z_2)}{\left[\int_{\mathcal{Z}} dz_1 \overline{\mathcal{N}}(z_1)\right]^2} \; , \quad (7)$$

where $\overline{\mathcal{N}}(z) \equiv \mathcal{N}(z)/r(z)$, $\mathcal{N}(z)$ is the actual redshift distribution of the catalogue and $r(z)$ describes the relation between the comoving radial coordinate and the redshift. In (7), $\xi_{\rm obj}(r,z_1,z_2)$ represents the correlation function of pairs of objects at redshifts $z_1$ and $z_2$ with comoving separation $r$, which can be safely approximated as $\xi_{\rm obj}(r,z_1,z_2) \approx b_{\rm eff}(z_1) b_{\rm eff}(z_2) \xi_{\rm m}(r,z_{\rm ave})$. Here $\xi_{\rm m}$ is the dark matter covariance function and $z_{\rm ave}$ is a suitably defined intermediate redshift (see Porciani 1997 for a discussion of possible choices).

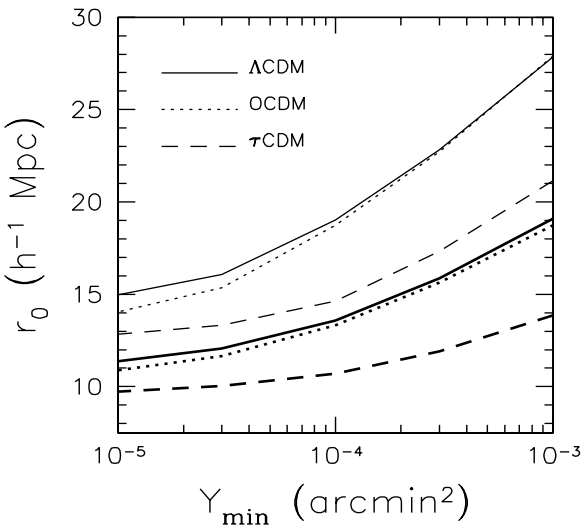


**Figure 1.** The dependence of the correlation length $r_0$ on the sensitivity limit $\overline{Y}_{\rm min}$ (in arcmin$^2$) is shown for $\Lambda CDM$ (solid lines), OCDM (dotted lines) and $\tau CDM$ models (dashed lines). Heavy lower and light upper lines refer cluster samples with $z < 0.3$ and $z > 0.3$, respectively.

A fundamental role in the previous equation is played by the effective bias $b_{\rm eff}$, which can be expressed as a weighted average of the 'monochromatic' bias factor $b(M,z)$ of objects with some given intrinsic property $M$ (like mass, luminosity, etc):

$$b_{\rm eff}(z) \equiv \mathcal{N}(z)^{-1} \int_{\mathcal{M}} d\ln M'\; b(M',z)\; \mathcal{N}(z,M') \, , \quad (8)$$

where $\mathcal{N}(z,M)$ is the number of objects actually present in the catalogue with redshift within $dz$ of $z$ and mass within $dM$ of $M$, whose integral over $\ln M$ is $\mathcal{N}(z)$.

In the case of galaxy clusters, it is possible to fully characterise their properties by the mass $M$ of their hosting dark matter haloes at each redshift $z$. This is consistent with the hierarchical model of structure formation where clusters are expected to form by merging of smaller mass units. The comoving mass function $\overline{n}(z,M)$ of dark matter haloes, required both in eq. (5) and in the computation of $\mathcal{N}(z,M)$, can be estimated using some extension of the Press-Schechter formalism. Moreover, we can adopt the Mo & White (1996) relation (or improvements thereof; see Sheth & Tormen 1999) for the monochromatic bias required in eq. (8). More precisely, we adopt the analytic relations obtained by Sheth & Tormen (1999; see also Sheth, Mo & Tormen 2001)

which are very well reproduced by the results of high-resolution $N$-body simulations (Jenkins et al. 2001).

For incorporating the fully non-linear regime, we use the fitting formula by Peacock & Dodds (1996) which allows the analytic computation of the redshift evolution of the dark matter covariance function $\xi_{\rm m}$. We also include the effects of redshift-space distortions using linear theory and the distant-observer approximation (Kaiser 1987).

Finally, in order to predict the abundance and clustering of galaxy clusters detected through their thermal SZ emission, we need to relate the expected characteristics of the samples (which in the case of SZ detected objects can be expressed in terms of the sensitivity limit $\overline{Y}_{\rm min}$) to a corresponding halo mass at each redshift. Such a relation is provided by the mass-temperature relation (eq. 4).

Changing the sensitivity limits, the characteristics of the detected cluster population change. In deep catalogues, faint objects (corresponding to low-mass haloes) can be detected. Due to the strong mass dependence of the monochromatic bias, a different clustering amplitude is expected. In Fig. 1 we show the dependence of the correlation length $r_0$ (defined as the scale where $\xi_{\rm obs}$ is unity) on the limits used to define the SZ surveys, i.e. the limiting sensitivity $\overline{Y}_{\rm min}$. The results are shown for galaxy clusters having $z < 0.3$ (heavy lower lines) and $z > 0.3$ (light upper lines) because at this redshift the expected *Planck* sample is roughly divided into two subsamples with a similar number of objects. We consider three different cosmological models, whose parameters are listed in Table 1. We find that $r_0$ is an increasing function of the limits defining a cluster survey: the larger $\overline{Y}_{\rm min}$ is, the more clustered the objects are, independent of the cosmological model. It is interesting to note that a similar trend was also predicted for galaxy clusters detected in the X-ray (Moscardini et al. 2000b) and optical bands (Moscardini et al. 2001).

## 4 COSMOLOGICAL IMPLICATIONS

We now discuss how the clustering properties of the SZ clusters depend on the cosmological parameters. We set the SZ sensitivity limit to that expected for the *Planck* satellite, i.e. $\overline{Y}_{\rm min} = 3 \times 10^{-4}$ arcmin$^2$. We will consider in detail three different cosmological models. They have a cold dark matter (CDM) power spectrum, a primordial power spectral index $n = 1$, and a shape parameter $\Gamma = 0.21$ in agreement with an extended set of observational data (e.g. Peacock & Dodds 1996). Moreover, they have the power-spectrum normalisation obtained by Viana & Liddle (1999) to reproduce the local cluster abundance. Notice that this normalisation has been challenged by very recent analyses, which, even if based on quite different approaches, seem to converge to substantially smaller values for $\sigma_8$ (Reiprich & Böhringer 2001; Viana, Nichol & Liddle 2001; Seljak 2001). Combined analyses of data coming from the 2dF Galaxy Redshift Survey and from measurements of the cosmic microwave background anisotropies seem to corroborate these low values of the power spectrum normalisation (Lahav et al. 2001). We will discuss later the effect of changing the assumed value for $\sigma_8$. The models correspond to different geometries. Specifically, we consider a flat model with matter density parameter $\Omega_{0\rm m} = 0.3$ and cosmological constant (hereafter $\Lambda$CDM); an open model with $\Omega_{0\rm m} = 0.3$ and vanishing cosmological constant (OCDM); and an Einstein-de Sitter model ($\tau$CDM). The two low-density models have a local Hubble constant $h \equiv H_0/(100{\rm km/s/Mpc}) = 0.7$, while we assume $h = 0.5$ for the $\tau$CDM model. The baryon fraction is set to $f_b = 0.075 h^{-3/2}$, as suggested by the analysis of X-ray data made by Mohr, Mathiesen & Evrard (1999). Table 1 summarises the model parameters.

**Table 1.** The parameters of the cosmological models. Column 2: the present matter density parameter $\Omega_{0\rm m}$; Column 3: the present cosmological constant contribution to the density $\Omega_{0\Lambda}$; Column 4: the primordial spectral index $n$; Column 5: the local Hubble parameter $h$; Column 6: the shape parameter $\Gamma$; Column 7: the spectrum normalisation $\sigma_8$; Column 8: the baryon fraction $f_b$.

| Model | $\Omega_{0\rm m}$ | $\Omega_{0\Lambda}$ | $n$ | $h$ | $\Gamma$ | $\sigma_8$ | $f_b$ |
|---|---|---|---|---|---|---|---|
| $\Lambda$CDM | 0.3 | 0.7 | 1.0 | 0.7 | 0.21 | 0.99 | 0.128 |
| OCDM | 0.3 | 0.0 | 1.0 | 0.7 | 0.21 | 0.84 | 0.128 |
| $\tau$CDM | 1.0 | 0.0 | 1.0 | 0.5 | 0.21 | 0.56 | 0.212 |

In the left panel of Figure 2 we show how the properties of the cluster population detectable for *Planck* change as a function of redshift. Locally objects with a relatively small mass will be detectable, of the order of galaxy groups: in fact $M_{\rm min} 10^{14}\ h^{-1}\ M_\odot$ for $z0.1$, independent of the cosmological model. At higher redshifts, the minimum mass increases: at $z \approx 0.5$ the *Planck* catalogue will include clusters with mass larger than $M_{\rm min} \approx 10^{14.6}\ h^{-1}\ M_\odot$ for low-density models and $M_{\rm min} \approx 10^{14.3}\ h^{-1}\ M_\odot$ for the Einstein-de Sitter model. Note that the differences between $\Lambda$CDM and OCDM are almost negligible. In fact the SZ clusters detected by *Planck* have relatively small redshifts, consequently the presence of the cosmological constant has small impact on the distance relations and the mass-temperature relation.

The right panel of Figure 2 presents the redshift dependence of the effective bias factor $b_{\rm eff}$. As expected, the bias is a strongly increasing function of $z$. This is due to two different reasons. First, the bias is itself an increasing function of mass, and we found an increase of $M_{\rm min}$ with redshift; second, even fixing the halo mass, the (squared) bias is inversely proportional to the clustering of the underlying dark matter distribution which is growing with time. This also explains the largest values of $b_{\rm eff}$ obtained for the $\tau$CDM model: in fact the growth factor is larger in an Einstein-de Sitter cosmology than in low-density models.

Figure 3 presents the predicted two-point correlation function $\xi_{\rm obs}$ computed for cluster samples having $z < 0.3$ and $z > 0.3$ (lower and upper lines, re-

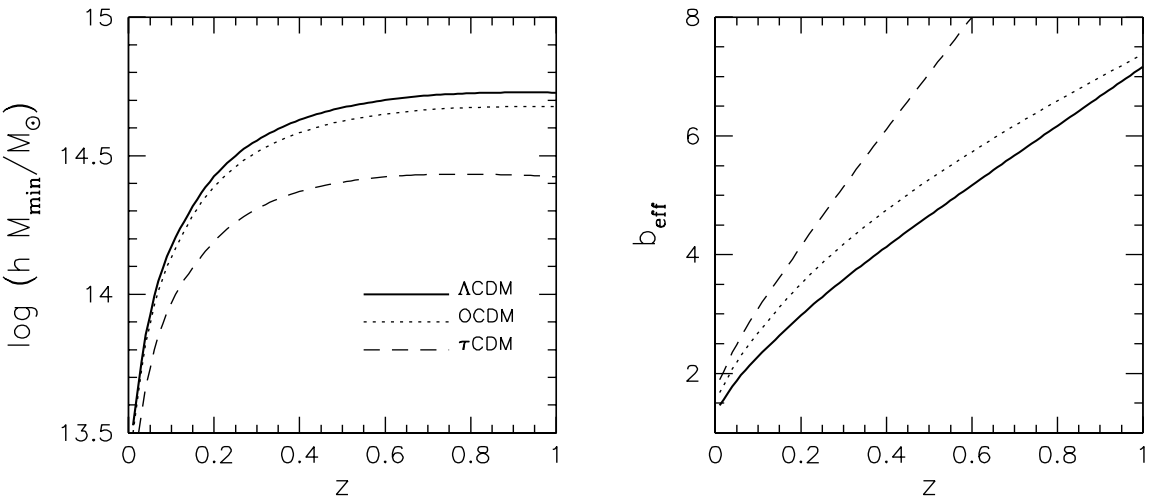


**Figure 2.** The minimum mass (left panel) and the effective bias factor (right panel) for clusters detectable for *Planck* are plotted as functions of redshift. Different line types refer to different cosmological models: $\Lambda CDM$ (solid lines), OCDM (dotted lines), $\tau CDM$ (dashed lines). The model parameters are summarised in Table 1.

spectively). In the plot 'mock-observational' 1-$\sigma$ error bars are given (only for the $\Lambda CDM$ model, for clarity). They are obtained by bootstrap resampling the number of expected pairs in each separation bin (Mo, Jing & Börner 1992). $\xi_{\rm obs}$ for the OCDM model is almost indistinguishable from the $\Lambda CDM$ case. This confirms that the clustering of SZ clusters is almost insensitive to the cosmological constant, as already found for objects detected in the X-ray and optical bands (see also the discussion of the following Figure 6). The predicted correlation function for the $\tau$CDM model is lower by approximately a factor of two, both for $z < 0.3$ and $z > 0.3$. The correlation lengths $r_0$ (still defined as the scales where $\xi_{\rm obs}$ is unity) for the low-redshift catalogues are $15.9 \pm 0.4$, $15.7 \pm 0.6$ and $11.9 \pm 0.2$ $h^{-1}$ Mpc for the $\Lambda$CDM, OCDM and $\tau$CDM models, respectively. As expected from the behaviour of the bias factor displayed in Figure 2, we find that the clusters are more clustered at higher redshift: the corresponding values of $r_0$ for the sample with $z > 0.3$ are $22.8 \pm 0.7$, $22.7 \pm 1.2$ and $17.3 \pm 1.1$ $h^{-1}$ Mpc, for $\Lambda$CDM, OCDM and $\tau$CDM models, respectively. Again, 1-$\sigma$ bootstrapping error estimates are given.

The differences expected between low- and high-density models are confirmed by the power-spectrum $P_{\rm obs}(k)$, which is shown in Fig. 4. Results are given for the cluster sample with $z < 0.3$ only. Again the differences between open and flat models with $\Omega_{0\rm m} = 0.3$ are negligible, while the power-spectrum for the $\tau CDM$ model is approximately a factor of two lower.

In order to better quantify the redshift evolution of clustering, we show in Fig. 5 the values of the correlation length computed using redshift bins of size $\Delta z = 0.2$ for the three cosmological models. From $z \approx 0$ to $z \approx 1$, $r_0$ changes by a factor of almost two. Locally the

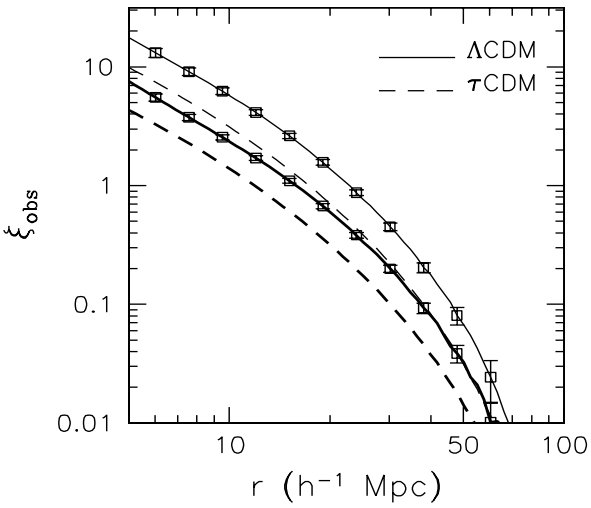


**Figure 3.** The spatial correlation function $\xi_{\rm obs}(r)$ is shown for clusters detectable for *Planck* with $z < 0.3$ (lower heavy lines) and $z > 0.3$ (upper light lines). The results refer to $\Lambda CDM$ and $\tau CDM$ models (solid and dashed lines, respectively). Results for OCDM are not shown because they are almost indistinguishable from the $\Lambda CDM$ model. Error bars (shown only for $\Lambda CDM$) are 1-$\sigma$ bootstrap estimates.

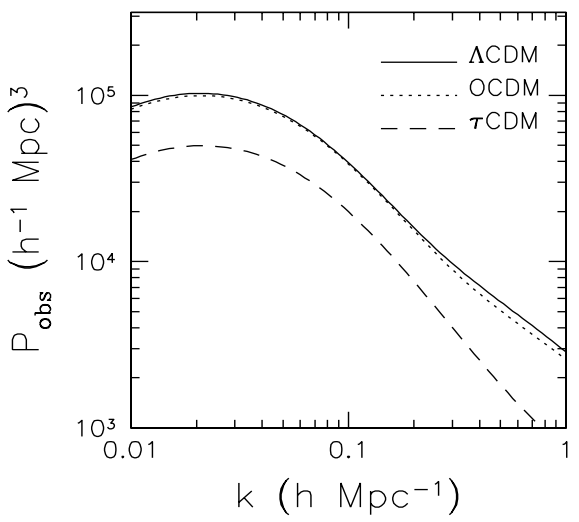


**Figure 4.** Theoretical predictions for the power-spectrum $P_{\rm obs}(k)$ are displayed for the *Planck* sample of SZ galaxy clusters. Results are presented for $\Lambda CDM$ (solid line), OCDM (dotted line) and $\tau CDM$ models (dashed line) and refer to clusters with $z < 0.3$ only.

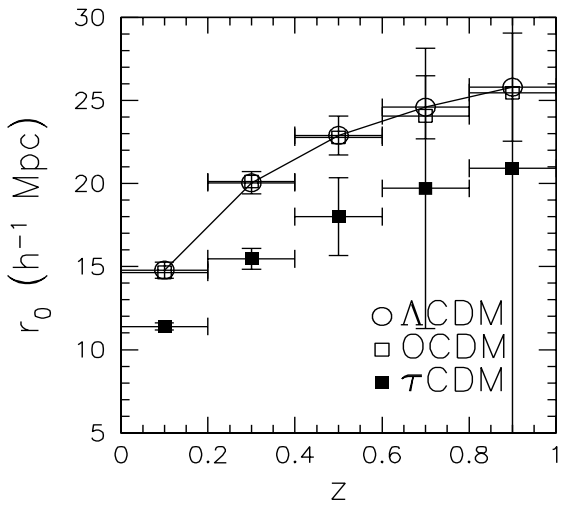


**Figure 5.** The redshift evolution of the correlation length $r_0$ is shown for $\Lambda CDM$ (open circles), OCDM (open squares) and $\tau CDM$ models (filled squares). Results are obtained dividing the expected cluster samples in redshift bins with size $\Delta z = 0.2$. Error bars (for clarity only shown for the $\Lambda CDM$ and $\tau CDM$ models) are 1-$\sigma$ bootstrap estimates.

SZ clusters detected by *Planck* are expected to have a correlation function only slightly larger than (local) galaxy groups or poor (optical) clusters. The predicted clustering signal at high redshift is quite large (albeit more uncertain due to the smaller number of objects) and can certainly be measured, at least in the case of low-density models. Note that, given its very large area, the *Planck* survey will be one of the best opportunities to measure the redshift evolution of cluster clustering. An alternative possibility (but in the X-ray band) will be the survey proposed for the XMM/Newton satellite (Refregier, Valtchanov & Pierre 2001). In this case the expected limiting flux will be approximately $S_{\rm lim} = 5 \times 10^{-15}$ erg cm$^{-2}$ s$^{-1}$ in the 0.5–2 keV band, but over a limited area of 64 square degrees.

So far, we considered models with fixed cosmological parameters. Now it is interesting to discuss the possibility of constraining these parameters using the clustering properties of *Planck* clusters. We start by considering the changes of the correlation length $r_0$ when the matter density parameter $\Omega_{0\rm m}$ is varied. The results are presented in Figure 6 for galaxy clusters with $z < 0.3$ and $z > 0.3$ (heavy and light lines, respectively). All models shown here have the spectrum normalisation required to reproduce the local cluster abundance. We use again the relation found by Viana & Liddle (1999), namely $\sigma_8 = 0.56\Omega_{0\rm m}^{-C}$, where $C = 0.34$ and $C = 0.47$ for open and flat models, respectively. Different choices for the normalisation will be discussed later. Primordial spectral index, shape parameter, Hubble parameter and baryon fraction are taken from Tab. 1. We find that varying $\Omega_{0\rm m}$ from 0.2 to 1.0 changes $r_0$ by 50 per cent for clusters with $z < 0.3$, and 30 per cent for clusters with $z > 0.3$. More precisely, the predicted correlation length decreases as $\Omega_{0\rm m}$ increases. Moreover, we notice that the cosmological constant increases the correlation length by less than 5%. In particular, at high redshifts the curves for flat and open models are almost identical. This is due to the relatively large value of the minimum mass of the detected clusters which implies the inclusion of objects with very similar properties. A similar result, i.e. the impossibility of constraining the presence of the cosmological constant using the clustering of galaxy clusters, was also found analysing cluster data in the optical and X-ray bands (Moscardini et al. 2000b; Moscardini, Matarrese & Mo 2001).

In Figure 7 we show how the correlation length $r_0$ changes when the spectrum normalisation $\sigma_8$ is varied. Again, results are shown for galaxy clusters with $z < 0.3$ and $z > 0.3$ (heavy and light lines, respectively). In the low-redshift bin, $r_0$ shows a small dependence on $\sigma_8$ and no significant differences are found using the Viana & Liddle (1999) normalisation compared to the more recent values obtained by Reiprich & Böhringer (2001), Seljak (2001) and Viana, Nichol & Liddle (2001). However, for clusters with $z > 0.3$ the variation is expected to be quite large. The predicted correlation length for low-density models changes from $r_0 \approx 35$ to $r_0 \approx 20h^{-1}$ Mpc as $\sigma_8$ is increased from 0.3 to 1.5. For the $\tau$CDM model the change is more limited: $r_0 \approx 23h^{-1}$ Mpc for $\sigma_8 = 0.3$ and $r_0 \approx 14 - 15h^{-1}$ Mpc for $0.7\sigma_8 < 1.5$. In particular, when the normalisation is changed from the largest value (Viana & Liddle 1999) to the lowest one (Viana et al. 2001), $r_0$ increases by roughly 20 per cent.

We also checked the effect on cluster clustering when only the Hubble parameter $h$ is varied, keeping all other parameters fixed as in Tab. 1 (the results are

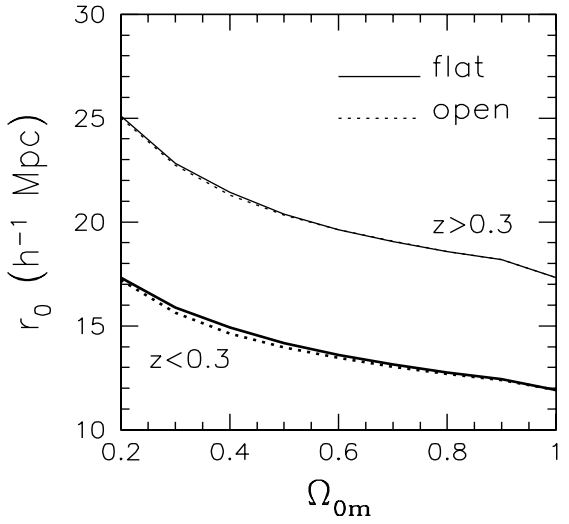


**Figure 6.** The predicted correlation length $r_0$ is plotted as a function of the present matter density parameter $\Omega_{0\mathrm{m}}$. Results are presented for CDM models with $\Gamma = 0.21$ and $\sigma_8$ chosen to reproduce the local cluster abundance (Viana & Liddle 1999). Solid lines: flat cosmological models (i.e. with non-zero cosmological constant); dotted lines: open models with vanishing $\Omega_{0\Lambda}$. Heavy lower and light upper lines refer to galaxy clusters with $z < 0.3$ and $z > 0.3$, respectively.

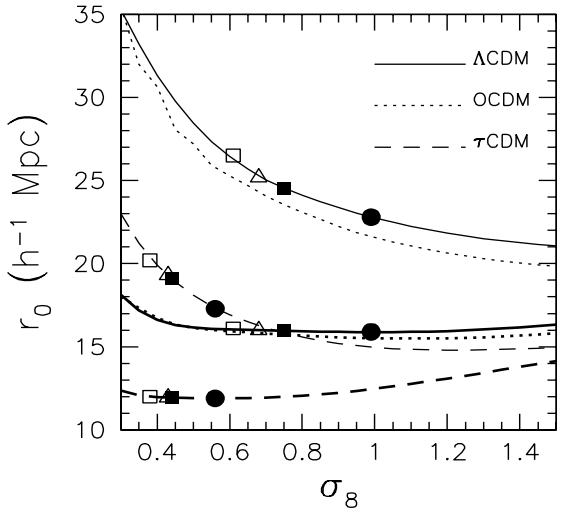


**Figure 7.** The predicted correlation length $r_0$ is shown as a function of the spectrum normalisation $\sigma_8$. Heavy lower and light upper lines refer to clusters with $z < 0.3$ and $z > 0.3$, respectively. Results are presented for $\Lambda CDM$ (solid lines), OCDM (dotted lines) and $\tau CDM$ models (dashed lines). Values of $r_0$ correspond to different estimates of $\sigma_8$ obtained by Viana & Liddle (1999), Seljak (2001), Reiprich & Böhringer (2001) and Viana, Nichol & Liddle (2001) are shown by solid circles, solid squares, open triangles and open squares, respectively.

not shown in the Figure). Varying $h$ from 0.4 to 1, the correlation length changes at most by 10%, independent of the cosmological model and redshift bin. This variation is certainly too small to allow any constraints on the Hubble constant.

## 5 DEPENDENCE ON THE PROPERTIES OF THE INTRACLUSTER MEDIUM

The SZ signal of galaxy clusters strongly depends on the properties of the intracluster medium. In fact the SZ signal reflects the distribution of hot gas in the clusters, as shown by eq. (1). So far, we employed a simple model: a baryon fraction fixed by the X-ray data of Mohr et al. (1999), a King profile for the gas distribution and a virial scaling relation between mass and temperature. In the following subsections we will study how sensitive the previous results are to these assumptions. Moreover, we will discuss if the clustering of SZ galaxy clusters can be used to directly constrain the properties of the intracluster medium.

### 5.1 Baryon fraction

In Figure 8 we show the dependence of the predicted correlation length $r_0$ on the baryon fraction $f_b$. We consider cluster samples with $z < 0.3$ and $z > 0.3$ (upper and lower panels, respectively), and two different cosmological models: $\Lambda CDM$ and $\tau CDM$ (left and right panels, respectively). We do not present results for OCDM because of their similarity with the $\Lambda CDM$ model. Three different relations between $f_b$ and the present Hubble parameter $h$ are assumed. First, we assume a perfect knowledge of the value of the Hubble constant: $h = 0.7$ and $h = 0.5$ for $\Lambda CDM$ and $\tau CDM$, respectively. Even if the second value appears to be too low when compared to recent observational estimates (e.g. Freedman et al. 2001), it is required in the case of an Einstein-de Sitter model to avoid a strong conflict between the age of the Universe and that of globular clusters. Second, we vary $h$ in agreement with the constraints from primordial nucleosynthesis: $f_b = 0.024/\Omega_{0\mathrm{m}}h^2$ (see e.g. the review by Schramm 1998). Finally we adopt again the relation given by Mohr et al. (1999) from the analysis of the X-ray data of 45 galaxy clusters. Notice that, given $f_b$, the values of $h$ corresponding to the previous relations can vary quite substantially. Consequently, the predicted scatter of $r_0$ indicates how well $f_b$ can be constrained with these clustering data.

In general we find small changes when we adopt the relations from primordial nucleosynthesis and X-ray data: the predicted values of $r_0$ differ only by 0.5-1 $h^{-1}$ Mpc for $0.05 f_b 0.25$, independent of the cosmological model. Thus, even with a well-determined correlation length, as expected with the *Planck* survey, only a rough estimate of the baryon fraction will be possible. The situation changes if we assume independent knowledge of the Hubble parameter $h$. Considering the expected 1-$\sigma$

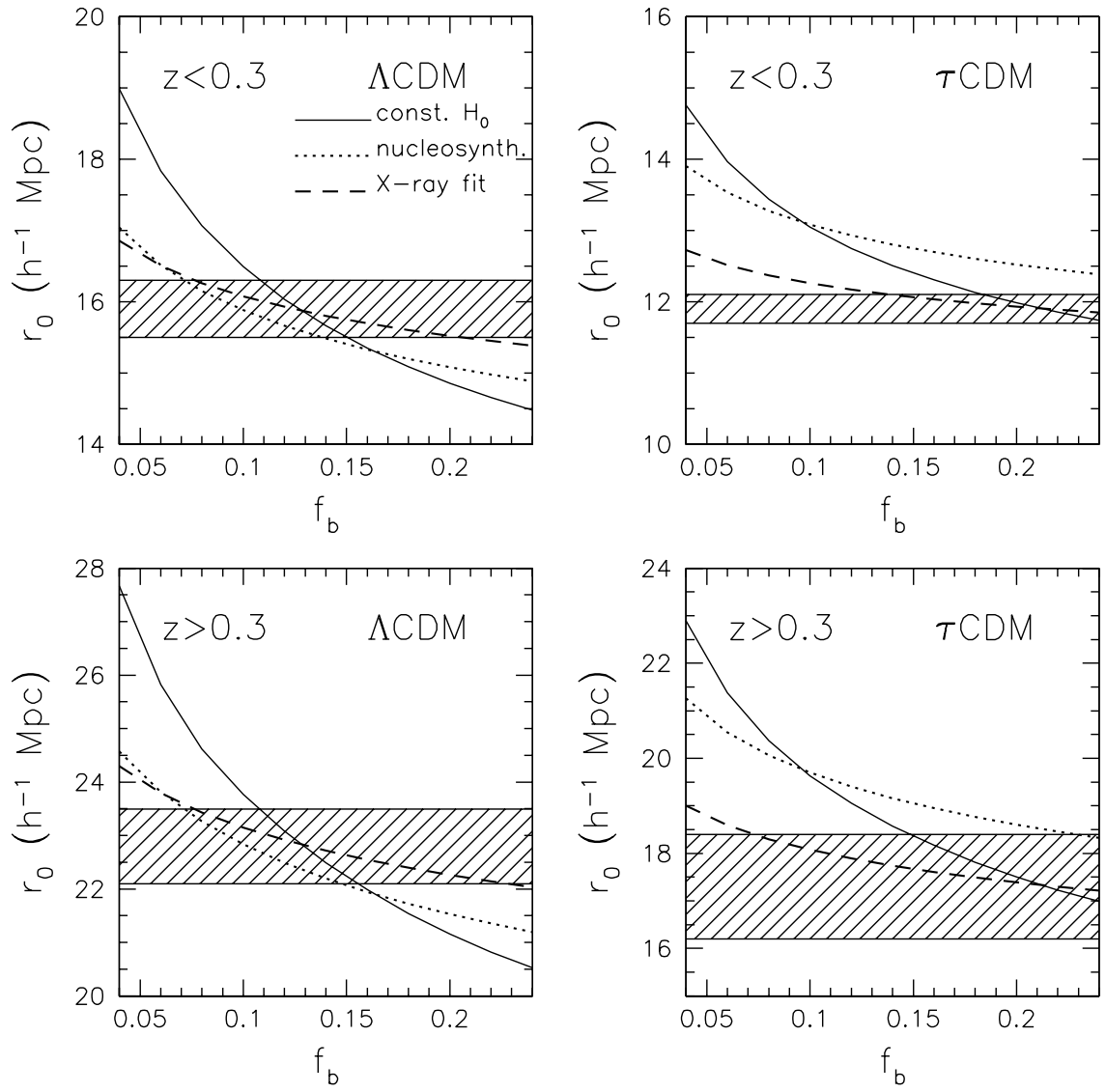


**Figure 8.** The predicted correlation length $r_0$ of galaxy clusters with $z < 0.3$ (upper panels) and $z > 0.3$ (lower panels) is plotted as a function of the baryon fraction $f_b$. Results are presented for the ΛCDM (left panels) and $\tau$CDM models (right panels). Different lines refer to different assumptions on the relation between the baryon fraction and the Hubble parameter $h$: constant $h$, equal to 0.7 and 0.5 for $\Lambda CDM$ and $\tau CDM$ models, respectively (solid lines); $f_b = 0.024/\Omega_{0\mathrm{m}}h^2$ as predicted from primordial nucleosynthesis (dotted lines); $f_b = 0.075h^{-3/2}$ as derived from X-ray data (dashed lines). The dashed regions show the 1-$\sigma$ ranges for $r_0$ as obtained using the parameters from Tab. 1.

error bars on $r_0$ for the low-redshift dataset, $f_b$ can be estimated from clustering data with typical uncertainties smaller than 0.02-0.03 for the $\Lambda CDM$ model and 0.05 for the $\tau CDM$ model. At higher redshifts ($z > 0.3$), one would expect a stronger dependence of the correlation length on the baryon fraction. In fact, if the value of $f_b$ is increased, clusters with lower mass are included in the *Planck* catalogue. Since the mass function is so steep, almost all clusters will have masses near the lower mass limit, which essentially determines the bias factor and consequently the correlation length. This is confirmed by our results: the change of $r_0$ with $f_b$ at high redshift is quite substantial (about 40 per cent across the plots). However, the expected 1-$\sigma$ error bars in the determinations of the correlation length increases in this redshift bin and the possibility to constrain $f_b$ remains roughly similar to the $z < 0.3$ dataset.

### 5.2 Dependence on the parameters of the mass-temperature relation

The results obtained so far were based on a fixed mass-temperature relation (eq. 4). The underlying assumptions are a virial isothermal distribution of gas and spherical collapse which are in discrete agreement both with numerical simulations (e.g. Bryan & Norman 1998; Frenk et al. 1999; Mathiesen & Evrard 2001) and observational estimates (Xu, Jin & Wu 2001; Finoguenov, Reiprich & Böhringer 2001). However the parameters in the relation are not well known. For example, different groups obtained different numerical values for the proportionality constant. Moreover, the presence of radiative cooling in cluster simulations changes both the normalisation and the slope of the mass-temperature relation (e.g. Muanwong et al. 2001). Finally also the redshift evolution of the relation, which cannot be constrained by present observational data, can be modified by different mechanisms, such as for instance the presence of an entropy floor (e.g. Tozzi & Norman 2001).

For testing the robustness of our previous results we will now study the variation of the correlation length $r_0$ in response to changes of the parameters in the mass-temperature relation. We modify eq. (4) as follows:

$$T = \alpha_1 \left( \frac{M}{10^{15} h^{-1} M_\odot} \right)^{\alpha_2} (1+z)^{\alpha_3} E^{2/3}(z) \left[ \frac{\Delta_{\rm vir}(z)}{178} \right]^{1/3} . \quad (9)$$

Here the parameters $\alpha_1$, $\alpha_2$ and $\alpha_3$ represent the normalisation, the slope of the relation and the exponent of the redshift dependence, respectively. The results of the previous section correspond to $(\alpha_1, \alpha_2, \alpha_3) = (6.03, 2/3, 0)$. The cosmological model is fixed to the $\Lambda CDM$ model (see Table 1).

Figure 9 shows the variation of the correlation length when only one parameter is changed. Results for clusters with $z < 0.3$ and $z > 0.3$ are presented in the left and right panels, respectively. For showing all curves in the same plots, we normalise the abscissa range using a parameter $\lambda$ defined as $\lambda \equiv (\alpha_i - \alpha_i^l)/(\alpha_i^h - \alpha_i^l)$, where $\alpha_i^l$ and $\alpha_i^h$ are the lower and upper limits of the considered range for the parameter $\alpha_i$. We consider the following intervals which are expected to cover the whole parameter region suggested by theoretical and numerical models: $3 \leq \alpha_1/\mathrm{keV} \leq 10$, $0.3 \leq \alpha_2 \leq 0.9$, $-1 \leq \alpha_3 \leq 1$. As expected, the redshift dependence ($\alpha_3$) is absolutely negligible in the low-redshift sample, but it also remains very weak for clusters with $z > 0.3$. The results are different when changing $\alpha_1$ and $\alpha_2$. Increasing the normalisation of the mass-temperature relation from 3 to 10 keV, $r_0$ is decreased from approximately 18 to $14.5h^{-1}$ Mpc for $z < 0.3$ and from approximately 26 to $21h^{-1}$ Mpc for $z > 0.3$. Similarly, when the slope $\alpha_2$ changes from 0.3 to 0.9, the correlation length increases from $\approx 13$ to $\approx 17h^{-1}$ Mpc for $z < 0.3$ and from $\approx 21$ to $\approx 23.5h^{-1}$ Mpc for $z > 0.3$. We recall that the predicted 1-$\sigma$ error bars for $r_0$ are 0.4 and 0.7 for the cluster samples at low- and high-redshift. Thus, using the clustering properties of SZ galaxy clusters to constrain cosmological parameters is hampered by our ignorance of the mass-temperature relation.

However, the dependence of $r_0$ on the details of the mass-temperature relation can be used to constrain them, once the cosmological model is known from alternative measurements (for instance, the analysis of the cosmic microwave background power-spectrum). To explore this possibility we allow the parameters to vary and compare with a maximum likelihood analysis the predicted correlation lengths to the results obtained using $(\alpha_1, \alpha_2, \alpha_3) = (6.03, 2/3, 0)$, which is our input parameter set. We recall that the corresponding correlation lengths are $r_0 = 15.9 \pm 0.4$ and $22.8 \pm 0.7 h^{-1}$ Mpc for clusters with $z < 0.3$ and $z > 0.3$, respectively. Since the previous results showed that the dependence on the redshift evolution parameter $\alpha_3$ is negligible, we decide to exclude it from the present analysis. Figure 10 shows the 68.3 and 95.4 per cent confidence levels for the samples of clusters with $z < 0.3$ (right panel), $z > 0.3$ (central panel) and for the combination of the two samples (right panel). Both at low and high redshift the normalisation and the slope of the mass-temperature relation appear to be strongly correlated, allowing large regions in the parameter space. This is expected: the same minimum mass can be obtained using different combinations of $\alpha_1$ and $\alpha_2$. When we combine the results of the two samples, the contours shrink and the parameters are better constrained. However the degeneracy between the two parameters does not permit their determination with (68.3 per cent) uncertainties less than 20 per cent.

## 6 CONCLUSIONS

In this paper we presented predictions for the clustering properties of galaxy clusters detectable through the thermal Sunyaev-Zel'dovich effect. In particular we showed results for surveys which are expected from the future *Planck* satellite, which will cover the whole sky down to a sensitivity limit of $\overline{Y}_{\rm min} = 3 \times 10^{-4}$ arcmin$^2$. Although our estimate of the sensitivity limit is quite conservative and very likely clusters of smaller mass or at higher redshift will be included into the real catalogue, the build up of a reliable cluster sample based on *Planck* data is not a straightforward process and requires large efforts, starting from the simultaneous

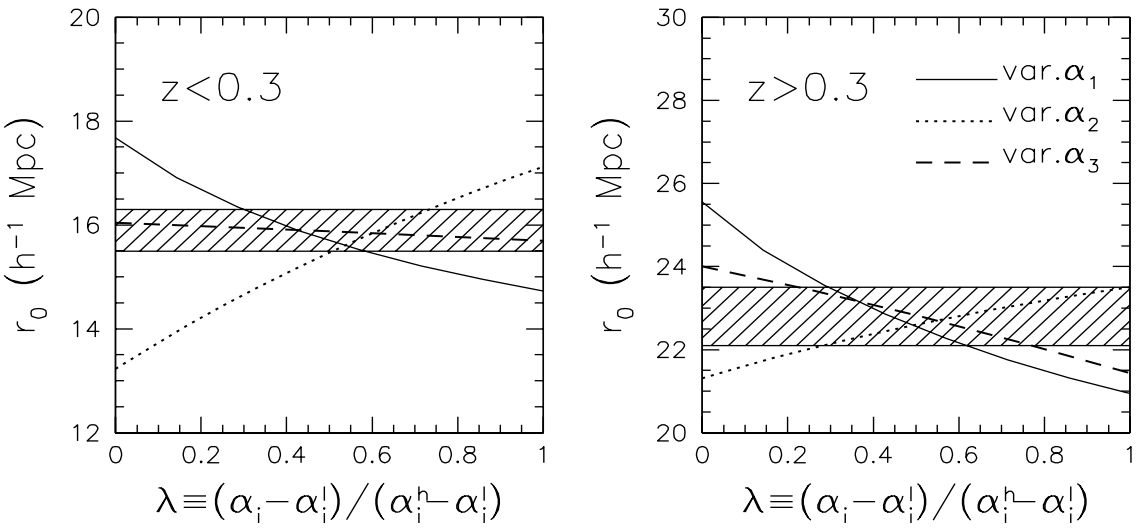


**Figure 9.** The variation in the predicted correlation length $r_0$ of galaxy clusters with $z < 0.3$ (left panel) and $z > 0.3$ (right panel) is shown in response to changes of the parameters $\alpha_i$ in the mass-temperature relation. The abscissa range is normalised using the parameter $\lambda$ defined as $\lambda \equiv (\alpha_i - \alpha_i^l)/(\alpha_i^h - \alpha_i^l)$, where $\alpha_i^l$ and $\alpha_i^h$ are the lower and upper limits for the parameter $\alpha_i$. The parameter $\alpha_1$ is the normalisation, ranging between 3 and 10 keV; $\alpha_2$ is the exponent of the mass, ranging between 0.3 and 0.9; and $\alpha_3$ is the exponent of the redshift dependence, ranging between -1 and 1. Results are presented for the $\Lambda CDM$ model only. The dashed regions show the 1-$\sigma$ ranges for $r_0$ as obtained using the parameters from Tab. 1.

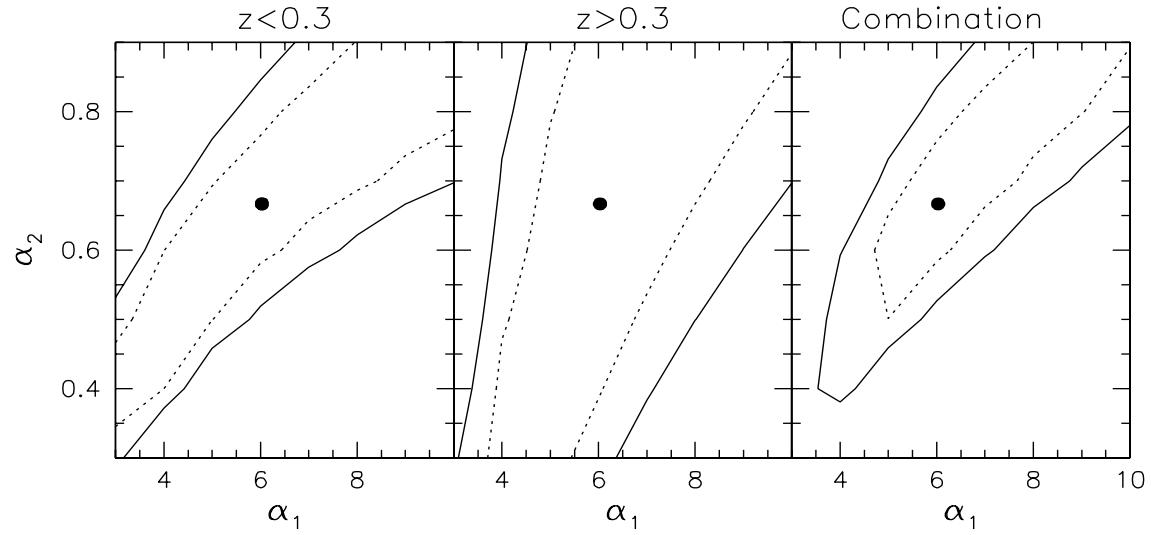


**Figure 10.** Confidence contours (68.3 and 95.4 per cent confidence levels; dotted and solid lines, respectively) are displayed for the normalisation ($\alpha_1$) and slope ($\alpha_2$) of the mass-temperature relation (see eq. 9); no redshift evolution is assumed here ($\alpha_3 = 0$). Results are given for the $\Lambda$CDM model only. Different panels refer to cluster samples with $z < 0.3$ (left panel), $z > 0.3$ (central panel) and to the combination of the two samples (right panel). Filled circles show the fiducial values of $\alpha_1 = 6.03$ and $\alpha_2 = 2/3$ which are the input parameters.

detection at (at least) two distinct frequencies of the enhancement and the decrement of the SZ signal and ending to the source identification and redshift determination. Despite these difficulties, it is worth stressing that *Planck* will give us a unique chance to construct an independent and unbiased galaxy cluster sample and to test cosmological scenarios. Here we showed, in fact, how it is possible to put independent constraints on some cosmological parameters and/or on physical properties of the intergalactic medium, on the basis of such a catalogue.

Our theoretical predictions were obtained for different cosmological scenarios using a model which accounts for the clustering of observable objects on our past light-cone and for the redshift evolution of both the underlying dark matter covariance function and the cluster bias factor. A linear treatment of redshift-space distortions was also included. Following an approach already applied to X-ray selected clusters, we make use of a theoretical relation between mass and temperature to convert the limiting sensitivity of a catalogue into the corresponding minimum mass for the dark matter haloes hosting the clusters. Based on this relation, the estimates for the clustering properties allow tests of the general scheme for the biased formation of galaxy clusters.

We found that the correlation length is an increasing function of the limits defining the surveys. A similar result was obtained in previous analyses of optical and X-ray selected clusters. When $\overline{Y}_{\rm min}$ is fixed to $3 \times 10^{-4}$ arcmin$^2$ as expected for *Planck*, the large number of detectable objects will allow a very accurate determination of the correlation length, with 1-$\sigma$ error bars of few per cent, much better than the existing estimates. Moreover the *Planck* cluster sample will extend to $z1$, giving the possibility to measure the redshift evolution of the correlation function. We found that the model predictions are depending on the main cosmological parameters, like the matter density parameter $\Omega_{0\rm m}$ and the power-spectrum normalisation $\sigma_8$, while the possible effect of the presence of a cosmological constant is almost negligible. However, the possibility of using future clustering data obtained by *Planck* to constrain the cosmological parameters is limited by the dependence of the results on the model adopted for the intracluster medium. For example, different assumptions on the baryon fraction produce variations of the correlation length similar to those found by changing $\Omega_{0\rm m}$. However, the dependence on $\sigma_8$ is strong enough for it to be constrained, in particular with high-redshift clusters (see Figure 7).

When a set of cosmological parameters is fixed, the cluster correlation function depends on the properties of the intracluster medium. We found that the *Planck* data can be used to constrain the baryon fraction with an accuracy of few per cent once the value of the Hubble constant is known. On the contrary, our results showed that the relation between mass and temperature, which parameterises the whole history of the physical processes inside the clusters, can only be poorly determined from clustering data alone.

**Acknowledgments.**

This work has been partially supported by Italian MIUR, CNR and ASI. We are grateful to Cristiano Porciani and Bepi Tormen for clarifying discussions. P.A. warmly thanks the IR group of the Max-Planck Institut fuer Extraterrestrische Physik in Garching for hospitality.

## REFERENCES

Abadi M.G., Lambas D.G., Muriel H., 1998, ApJ, 507, 526
Aghanim N., De Luca A., Bouchet F.R., Gispert R., Puget J.-L., 1997, A&A, 325, 9
Bartelmann M., 2001, A&A, 370, 754
Bartlett J., 2000, preprint, astro-ph/0001267
Borgani S. et al., 2001, ApJ, 561, 13
Borgani S., Plionis M., Kolokotronis V., 1999, MNRAS, 305, 866
Bryan G.L., Norman M.L., 1998, ApJ, 495, 80
Collins C.A. et al., 2000, MNRAS, 319, 939
Croft R.A.C., Dalton G.B., Efstathiou G., Sutherland W.J., Maddox S.J., 1997, MNRAS, 291, 305
Eke V.R., Cole S., Frenk C.S., Henry P.J., 1998, MNRAS, 298, 1145
Finoguenov A., Reiprich T.H., Böhringer H., 2001, A&A, 368, 749
Freedman W.L. et al., 2001, ApJ, 553, 47
Frenk C.S. et al., 1999, ApJ, 525, 554
Haehnelt M.G., 1997, in Bouchet F.R. et al. eds., Microwave Background Anisotropies. Gif-sur-Yvette: Editions Frontières
Hamana T., Yoshida N., Suto Y., Evrard A.E., 2001, ApJ, in press, astro-ph/0110061
Hobson M.P., Jones A.W., Lasenby A.N., Bouchet F.R., 1998, MNRAS, 300, 1
Jenkins A., Frenk C.S., White S.D.M., Colberg J.M., Cole S., Evrard A.E., Yoshida N., 2001, MNRAS, 321, 372
Kaiser N., 1987, MNRAS, 227, 1
Komatsu E., Kitayama T., 1999, ApJ, 526, L1
Lahav O. et al., 2001, preprint, astro-ph/0112162
Matarrese S., Coles P., Lucchin F., Moscardini L., 1997, MNRAS, 286, 115
Mathiesen B.F., Evrard A.E., 2001, ApJ, 546, 100
Mo H.J., Jing Y.P., Börner G., 1992, ApJ, 392, 452
Mo H.J., White S.D.M., 1996, MNRAS, 282, 347
Mohr J.J., Mathiesen B.F., Evrard A.E., 1999, ApJ, 517, 627
Moscardini L., Coles P., Lucchin F., Matarrese S., 1998, MNRAS, 299, 95
Moscardini L., Matarrese S., De Grandi S., Lucchin F., 2000a, MNRAS, 314, 647
Moscardini L., Matarrese S., Lucchin F., Rosati P., 2000b, MNRAS, 316, 283
Moscardini L., Matarrese S., H.J. Mo, 2001, MNRAS, 327, 422
Muanwong P. Thomas P.A., Kay S.T., Pearce F.R., Couchman H.M.P., 2001, ApJ, 552, L27
Nichol R.C., Collins C.A., Guzzo L., Lumsden S.L., 1992, MNRAS, 255, 21p
Peacock J.A., Dodds S.J., 1996, MNRAS, 280, L19
Porciani C., 1997, MNRAS, 290, 639
Refregier A., Komatsu E., Spergel D.N., Pen U.-L., 2000, Phys. Rev., D11, 123001
Refregier A., Valtchanov I., Pierre M., 2001, preprint, astro-ph/0109529

Reiprich T.H, Böhringer H., 2001, preprint, astro-ph/0111285
Sadat R., Blanchard A., Oubkir J., 1998, A&A, 329, 21
Schramm D.N., 1998, in Olinto A.V., Frieman J.A. & Schramm D.N. eds., Proc. of 18th Texas Symposium on Relativistic Astrophysics and Cosmology. Singapore: World Scientific
Schuecker P. et al., 2001, A&A, 368, 86
Seljak U., 2001, preprint, astro-ph/0111362
Sheth R.K., Mo H.J., Tormen G., 2001, MNRAS, 323, 1
Sheth R.K., Tormen G., 1999, MNRAS, 308, 119
Suto Y., Yamamoto K., Kitayama T., Jing Y.P., 2000, ApJ, 534, 551
Tozzi P., Norman C., 2001, ApJ, 546, 63
Verde L., Haiman Z., Spergel D.N., 2001, preprint, astro-ph/0106315
Viana P.T.P., Liddle A.R., 1999, MNRAS, 303, 535
Viana P.T.P., Nichol R.C., Liddle A.R., 2001, preprint, astro-ph/0111394
Xu H., Jin G., Wu X.-P., 2001, ApJ, 553, 78
Yamamoto K., Suto Y., 1999, ApJ, 517, 1